Eur. Phys. J. D **45**, 309–315 (2007)
DOI: 10.1140/epjd/e2007-00254-x

THE EUROPEAN PHYSICAL JOURNAL D

Monte Carlo simulations of electron dynamics in N_2/CO_2 mixtures

M. Janda[1,a], V. Martišovitš[2], M. Morvová[2], Z. Machala[2], and K. Hensel[2]

[1] École Centrale Paris, Laboratoire EM2C - CNRS UPR 288, Grande Voie des Vignes, 92290 Châtenay-Malabry, France
[2] Comenius University, Faculty of Mathematics, Physics and Informatics, Department of Astronomy, Earth Physics and Meteorology, Mlynská dolina F2, 842 48 Bratislava, Slovakia

Received 11 May 2007 / Received in final form 19 July 2007
Published online 31 August 2007 –

Abstract. Motivated by experimental investigations of electrical discharges in $N_2/CO_2/H_2O$, Monte Carlo (MC) electron dynamics simulations in atmospheric N_2/CO_2 mixtures were performed. The goal was to obtain electron energy distribution functions (EEDFs), mean free path, drift velocity, collision frequency and mean energy of electrons, rate coefficients of electron-impact reactions, ionisation and attachment coefficients, as functions of the reduced electric field strength (E/N) and of the concentration of individual gas components. The results obtained by MC simulations were fitted with polynomials of up to the 3rd order with reasonable accuracy for E/N above 80 Td. The studied parameters below 80 Td were strongly non-linear as functions of E/N. This is mostly due to the influence of elastic collisions of electrons with CO_2 molecules prevailing in CO_2-dominant mixtures for $E/N < 40$ Td, and vibrational excitation collisions of N_2 species prevailing in N_2-dominant mixtures for E/N from 40 to 80 Td. The effect of these electron-impact processes was specific for each of the studied parameters.

PACS. 52.65.Pp Monte Carlo methods – 02.50.Ng Distribution theory and Monte Carlo studies – 51.50.+v Electrical properties (ionisation, breakdown, electron and ion mobility, etc.)

1 Introduction

Plasma, unlike gases that are usually chemically inert at standard conditions, posses chemical activity due to electrons, excited particles, ions and radicals present. Chemical effects of plasmas generated by various types of electrical discharges operating in many gaseous mixtures have been extensively investigated during the last few decades [1,2]. Such plasmas can be applied for ozone generation, exhaust gas and waste water treatment, chemical synthesis, CO_2 utilisation, surface modifications, removal of hazardous compounds, bio-decontamination, etc. [3–6].

Chemistry induced by atmospheric pressure DC electrical discharges in $N_2/CO_2/H_2O$ mixtures was studied recently [7–10]. This mixture represents a model prebiotic atmosphere of the Earth and a simplified flue gas from the stoichiometric combustion of the natural gas. The aim of these studies was the decomposition of CO_2, which is the dominant contributor to the enhanced greenhouse effect, and the formation of organic species, especially amino acids. Synthesis of some essential amino acids was detected by electrical discharges, which is very interesting from the viewpoint of the theory of origins of life. The mechanism of synthesis of amino acids from simple inorganic molecules is still not completely understood.

Generally, a detailed description of the reaction mechanisms in plasmas is a complicated task. However, it is well-known that high energy electrons accelerated in an electric field represent the key initiating factor in electrical discharges inducing low-temperature plasma chemistry. For this reason we show here calculations of the rate coefficients of electron-impact reactions in N_2/CO_2 mixtures. Next, we plan to study the influence of humidity on these rate coefficients in $N_2/CO_2/H_2O$ mixtures.

The calculation of the rate coefficients for electron-impact reactions requires the knowledge of electron energy distribution functions (EEDFs). The EEDF, $f(\varepsilon)$, can be defined in such a way that the local fraction of electrons in the energy range $(\varepsilon, \varepsilon + \mathrm{d}\varepsilon)$ is given by $f(\varepsilon)\,\varepsilon^{1/2}\,\mathrm{d}\varepsilon$. In cold plasmas, EEDFs may have strongly non-Maxwellian shape but they satisfy the Boltzmann equation. Thus, one way to obtain EEDFs is to solve numerically simplified versions of the Boltzmann equation. The second approach is to use Monte Carlo (MC) methods that are widely used for complex physical and mathematical problems.

The examples of the utilization of MC methods can be also found in the fields of both low and high temperature plasmas. The MC methods were used for example for the modelling of edge plasma and plasma surface interactions in fusion experiments [11–13], or for the simulation of low energy electrons and photons interactions [14]. The MC algorithms can be also used to compute a trajectory

[a] e-mail: mario.janda@em2c.ecp.fr

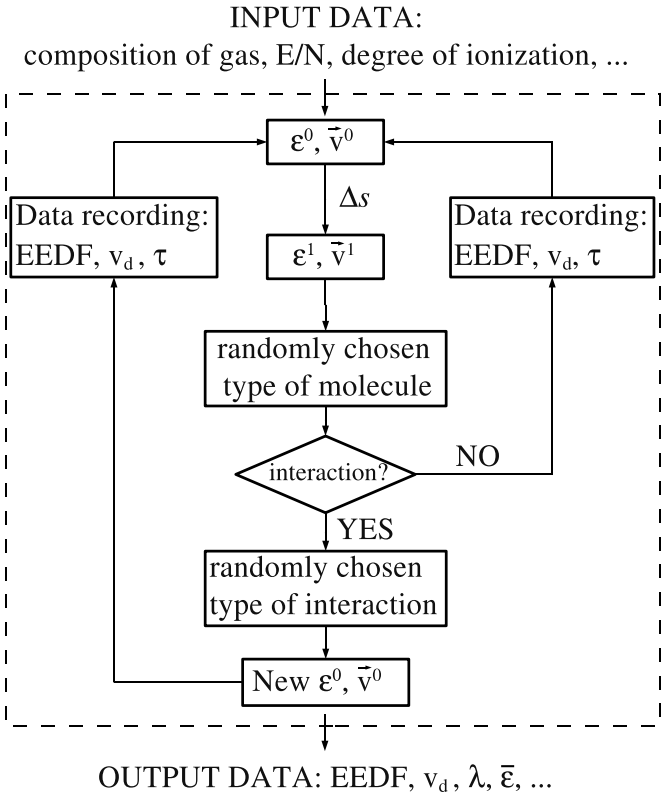

Fig. 1. Schematic of the algorithm used in Web-EEDF.

of electrons [15–19]. The so-called 'zero-collision' MC method, originally developed by Skullerud [20], is frequently used to compute plasma parameters, see [21,22]. This algorithm, based on collisional frequencies of the electron, is currently mostly used for noble gases. The so-called particle-in-cell method has been applied to RF discharges by Birdsall [23] and Sommeren [24].

The similarity of results obtained by MC methods and the numerical solution of the Boltzmann equation was shown by Segur et al. [25], although the authors stressed the necessity of using more than the first four terms of the spherical harmonic expansion in the solution of the Boltzmann equation. We decided to use MC simulation of electron dynamics to calculate EEDFs in the studied gas mixtures. For this purpose, we developed an open source software named 'Web-EEDF' [26,27], based on the algorithm presented by Tas et al. [28]. The reliability of our results was proved by their comparison with data found in literature [26,29].

2 Algorithm

The EEDF is usually defined as the energy distribution of an assembly of n electrons at time t. Our algorithm (Fig. 1) is based on the presumption, that the same EEDF is found when the energy of a single electron is sampled at n moments in time (ergodic theory). We follow a single electron as it moves in the studied gas mixture and we record its energy and several further characteristics in n computational cycles. The energy of the electron and the direction of its motion changes during the simulation, due to its acceleration by an electric field and due to its interaction with other species (atoms, molecules, background electrons). There are three types of electron interactions implemented:

1. elastic electron-molecule (atom) collisions,
2. inelastic electron-molecule (atom) collisions,
3. electron-electron interactions.

The composition of the gas, its pressure (p) and temperature (T_g), the reduced electric field strength (E/N), the initial temperature of electrons (T_e), the number of computational cycles (n), and the degree of ionisation (ξ) which is defined as the ratio of electron and neutral densities, are taken as initial parameters in our algorithm. The initial energy of the test electron is randomly chosen from the Maxwellian distribution given by T_e. The direction of its motion relative to the electric field vector $\boldsymbol{E}$ is chosen randomly as well. Afterwards, the motion of the test electron is followed in a required number of computational cycles. Within one computational cycle, the electron is accelerated over a distance Δs, which is equal to the average distance between molecules at the given p and T_g, and its new energy and new direction of its motion are calculated. The direction is determined by the velocity vector $\boldsymbol{v}$, which has two components: parallel ($v_\parallel$) and perpendicular ($v_\perp$) to $\boldsymbol{E}$. This is the most important feature in our algorithm compared to the original algorithm of Tas et al. [28], where the electron movement was straightforward along $\boldsymbol{E}$, and its acceleration over Δs was approximated by a parametrisation.

During each cycle, after the electron changes its position by the distance Δs, a random number determines the type of molecule with which the electron may interact. Another random number determines whether the electron will really interact with this molecule or not and the type of this interaction. The probability of each type of interaction depends on its cross section. We used the compilation of cross sections obtained from Joint Institute for Laboratory Astrophysics (JILA) [30], with the update for CO_2 cross sections according to Itikawa [31].

If the interaction occurs, the energy of electron is decreased by $\Delta\varepsilon$ and a new direction of its motion is chosen randomly. The value of $\Delta\varepsilon$ depends on the type of this interaction. In case of the elastic scattering, $\Delta\varepsilon$ is taken equal to average momentum transfer: $\Delta\varepsilon = 2m_e\varepsilon/M$, where m_e and M are the masses of the electron and neutral species, respectively. The excitation of a molecule decreases the energy of the test electron by the amount of energy required to excite the molecule (ε^{exc}): $\Delta\varepsilon = -\varepsilon^{exc}$. In case of ionization, electron loses the energy which is required to ionize the molecule (ε^{ion}), plus its remaining energy is shared randomly between itself and the second electron released by the ionized species. The released electron is not further considered in the calculations.

As we assumed an isotropic scattering, the orientation of the electron's motion after each collision is random. However, the momentum transfer cross sections (q_m)

that we use include some anisotropic effects. By definition, a large angle scattering contributes to q_m more than a small angle scattering. Moreover, the typical probability of the interaction of the test electron with neutrals during each cycle is around 1% at atmospheric pressure and room temperature in N_2/CO_2 mixture. It means that there is approximately 100 computational cycles with no collision per 1 cycle with a collision. Thus, we minimize the influence of the initial random direction of the electron motion after each collision on EEDF by a large number of 'zero-collisional' cycles between collisions.

If the interaction of the test electron with neutral species does not occur and $\xi > 0$, the possibility of interaction with a background electron is tested by another random number. The electron-electron interaction is described by so-called Coulomb cross section taken from Mitchner and Kruger [32], and the energy exchange between these electrons is approximated by the scheme of Weng and Kushner [21].

The energy of the electron, the direction of its motion, and the time since its last collision (τ) are stored after each computational cycle, regardless an interaction occurs or not. At the end of the simulation, after n computational cycles, the obtained EEDF is normalised so that $\int_0^\infty f(\varepsilon)\sqrt{\varepsilon}\,\mathrm{d}\varepsilon = 1$. Final results include the electron drift velocity (v_d), the electron mean energy ($\bar{\varepsilon}$), the collision frequency of electrons with neutrals (ν), the electron mean free path (λ), the electron mobility, the rate coefficients of electron-impact reactions and the branching of the electron energy towards various electron-impact processes. It is further possible to use these data to calculate additional parameters. For example, we present here the calculation of ionisation (α) and attachment (η) coefficients that are defined as follows:

$$\alpha = k_{ion} N / v_d \tag{1}$$

$$\eta = k_{att} N / v_d \tag{2}$$

where k_{ion} is the rate coefficient for electron-impact ionisation, N is the density of neutrals in cm^{-3}, k_{att} is the rate coefficient for electron attachment reactions. These coefficients represent the increase or the decrease in electron density per centimetre resulting from ionisation and attachment, respectively. The ionization coefficient is also known as the first Townsend coefficient.

2.1 Computational conditions

The value of E/N varied from 10 to 400 Td (1 Td = 10^{-17} V cm^2) and the concentration of CO_2 varied from 0 to 100 vol.% during our simulations. Calculations were performed at normal conditions (pressure 10^5 Pa and gas temperature 293 K). The initial electron temperature was also 293 K. The degree of ionisation was set to zero ($\xi = 0$), i.e. we neglected electron-electron interactions. According to our previous calculations [26], this simplification is correct for plasmas with $\xi < 10^{-4}$, corresponding to the concentration of electrons (n_e) below 2.5×10^{15} cm^{-3} at normal conditions. At higher electron densities, the curves of the EEDF tends towards Maxwellian distribution due to the electron-electron interactions [28].

All simulations were performed with 20 million computational cycles. This number is a good compromise between the accuracy of the obtained data and the computational time [29]. In order to obtain accurate values of $\bar{\varepsilon}$, v_d, λ and ν, even 5 million cycles would be enough, but the rate coefficients of reactions with a high threshold energy (ε_{th}) require at least 20 million computational cycles. The reason is in the statistics: parameters such as $\bar{\varepsilon}$, v_d, λ and ν were calculated from the whole EEDF, whereas rate coefficients were calculated only from its 'tail' above the ε_{th}. The standard deviations of the mean values of the rate coefficients calculated in ten runs at 60, 100, and 140 Td showed that the accuracy decreases with the increasing ε_{th} and with the decreasing value of E/N. At 60 Td, the deviation for processes with $\varepsilon_{th} > 12$ eV was more than 50%. At 100 Td, only the rate coefficient for the ionisation of N_2, with $\varepsilon_{th} = 15.6$ eV, performed the deviation approaching 50%. Above 140 Td, all the rate coefficients had deviations below 10%. The deviations of $\bar{\varepsilon}$, v_d, λ, ν did not depend on E/N and they were below 1.5% [29].

3 Results and discussion

There are dozens of possible reactions that can result from the electron interaction with N_2 and CO_2 molecules. The elastic scattering of electrons and vibrational excitations of N_2 and CO_2 molecules are the fastest electron-impact processes, but they do not directly influence the plasma chemistry. Here, we present only the calculated rate coefficients of the electron-impact reactions, which we consider to be the most important for plasma chemistry and generation of electrical discharges in N_2/CO_2 mixture. Namely, the reactions leading to the dissociation of N_2 and CO_2 (Eqs. (7) and (4)), the production of metastable $N_2(A^3\Sigma_u^+)$ species, (Eq. (5)), and the electron-impact ionisation and attachment (Eqs. (3), (9), and (10)). The metastable $N_2(A^3\Sigma_u^+)$ species may also be generated by the radiative de-excitation cascade from $N_2(B^3\Pi_g)$ and $N_2(C^3\Pi_u)$ species, produced primarily by electron-impact reactions (Eqs. (6) and (8))

$$e + CO_2 \rightarrow CO + O^- \qquad \varepsilon_{th} = 3.9 \text{ eV} \tag{3}$$

$$e + CO_2 \rightarrow CO_2(a^3\pi) + e \qquad \varepsilon_{th} = 6.1 \text{ eV} \tag{4}$$

$$e + N_2 \rightarrow N_2(A^3\Sigma_u^+) + e \qquad \varepsilon_{th} = 6.17 \text{ eV} \tag{5}$$

$$e + N_2 \rightarrow N_2(B^3\Pi_g) + e \qquad \varepsilon_{th} = 7.35 \text{ eV} \tag{6}$$

$$e + N_2 \rightarrow N + N + e \qquad \varepsilon_{th} = 10.0 \text{ eV} \tag{7}$$

$$e + N_2 \rightarrow N_2(C^3\Pi_u) + e \qquad \varepsilon_{th} = 11.03 \text{ eV} \tag{8}$$

$$e + CO_2 \rightarrow CO_2^+ + 2e \qquad \varepsilon_{th} = 13.3 \text{ eV} \tag{9}$$

$$e + N_2 \rightarrow N_2^+ + 2e \qquad \varepsilon_{th} = 15.6 \text{ eV}. \tag{10}$$

We refer to an individual rate coefficient by the number of the specific reaction, e.g. k_7 is the rate coefficient of the reaction (7). Besides these rate coefficients, we present $\bar{\varepsilon}$, v_d, ν, λ, α, and η.

3.1 Fitting of calculated parameters

The EEDF and the derived parameters depend on E/N and the composition of the mixture, determined for example by the concentration of nitrogen (δ_{N_2}). In order to describe the changes of the studied parameters as functions of E/N and δ_{N_2}, we fitted them. In the first step, we fitted them by polynomials of up to the 3rd order, as functions of δ_{N_2} at fixed values of E/N:

$$\Phi\left(\frac{E}{N}, \delta_{N_2}\right) = a_0 + a_1\delta_{N_2} + a_2(\delta_{N_2})^2 + a_3(\delta_{N_2})^3. \quad (11)$$

Here, Φ represents any of presented parameters ($\lambda, \nu, \ldots$). Thus we obtained a set of fitting coefficients a_i, which were subsequently fitted by the polynomials of up to the 3rd order, as functions of E/N:

$$a_i\left(\frac{E}{N}\right) = b_{i0} + b_{i1}\left(\frac{E}{N}\right) + b_{i2}\left(\frac{E}{N}\right)^2 + b_{i3}\left(\frac{E}{N}\right)^3. \quad (12)$$

Finally, we obtained a set of fitting coefficients b_{ij}, which enable to calculate the value of each studied parameters by the following formula:

$$\Phi\left(\frac{E}{N}, \delta_{N_2}\right) = \left(1, \left(\tfrac{E}{N}\right)^1, \ldots, \left(\tfrac{E}{N}\right)^{m-1}\right) \mathbf{B}_\Phi \begin{pmatrix} 1 \\ (\delta_{N_2})^1 \\ \vdots \\ (\delta_{N_2})^{n-1} \end{pmatrix} \quad (13)$$

where $\boldsymbol{B}_\Phi$ is a matrix of $m \times n$ type with fitting coefficients b_{ij}. If m or n are smaller than 4, it was not necessary to use polynomials of the 3rd order to fit the parameter Φ. On the other hand, it was not possible to fit all coefficients a_i with sufficient accuracy in the whole range of E/N even with polynomials of the 3rd order.

The differences between the values of the studied parameters obtained by MC simulations (Φ_{MC}) and their values calculated from the fitting coefficients (Φ_{fit}) were also evaluated. The average differences between Φ_{MC} and Φ_{fit} defined as

$$\Delta = \frac{|\Phi_{MC} - \Phi_{fit}|}{\Phi_{MC}} 100\ [\%] \quad (14)$$

for various values of E/N are summarised in Table 1, where the corresponding range of E/N for which the given fitting coefficients may be applied can be also found. The fitting coefficients themselves can be downloaded from `http://enviro.fmph.uniba.sk/web-eedf`.

3.2 Mean energy of electrons

For $E/N < 25$ Td, the electron mean energy $\bar{\varepsilon}$ was determined mostly by the large momentum transfer cross section of CO_2. In stronger fields, the influence of cross sections for vibrational excitation of N_2 dominated. This influence was the strongest at around 40 Td, where even in the mixture with 50% of CO_2, the value of $\bar{\varepsilon}$ was almost identical with the value in pure N_2 (Fig. 2). For $E/N \geq 40$ Td, the value of $\bar{\varepsilon}$ grew monotonously with the deceasing δ_{N_2}. For $E/N \geq 80$ Td, this growth was approximately linear and it was possible to fit $\bar{\varepsilon}$ according to equations (11–13).

Table 1. The range of applicability of obtained fitting coefficients and average differences between the results obtained by MC simulations and those obtained by using the fitting coefficients for different values of E/N ($\langle\Delta_{E/N}\rangle$).

Parameter	Applicability [Td]	$\langle\Delta_{E/N}\rangle$ [%] 80 Td	120 Td	200 Td
$\bar{\varepsilon}$	80–400	3.1	1.0	1.0
v_d	80–400	5.5	5.5	3.4
ν	60–400	2.8	1.9	1.8
λ	60–400	1.3	1.1	1.0
k_3	80–400	4.5	2.3	0.8
k_4	80–400	10.4	1.4	1.0
k_5	80–400	8.1	9.0	2.0
k_6	80–400	11	2.4	1.5
k_7	100–400	–	9.2	2.8
k_8	120–400	–	14	2.6
k_9	120–400	–	12	8.3
k_{10}	120–400	–	23	7.5

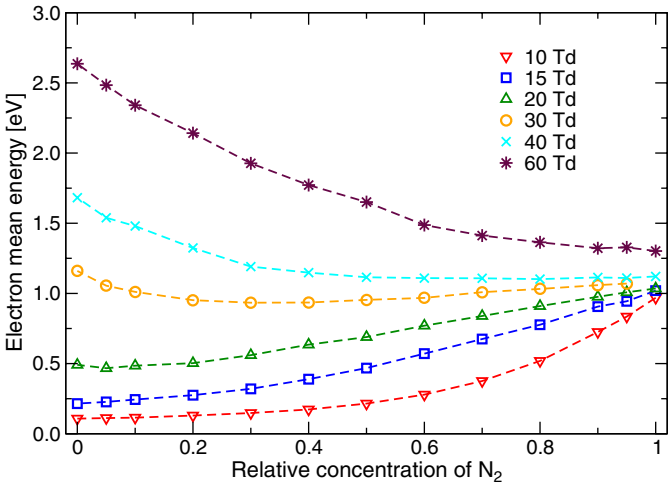

Fig. 2. Electron mean energy in N_2/CO_2 mixture for $E/N < 80$ Td.

3.3 Drift velocity of electrons

The changes of v_d due to the changes of δ_{N_2} were also nonlinear for E/N below 80 Td. Their character, however, was different compared to $\bar{\varepsilon}$, since the maximum v_d did not occur in pure gases but in the mixtures with certain values of δ_{N_2}, depending on E/N (Fig. 3). For $E/N \geq 80$ Td, v_d changed linearly with the increasing δ_{N_2}, and it was possible to fit it according to equations (11–13). For E/N below 300 Td, v_d decreased with the increasing δ_{N_2}, though the slope of this decrease diminished with the increase of E/N.

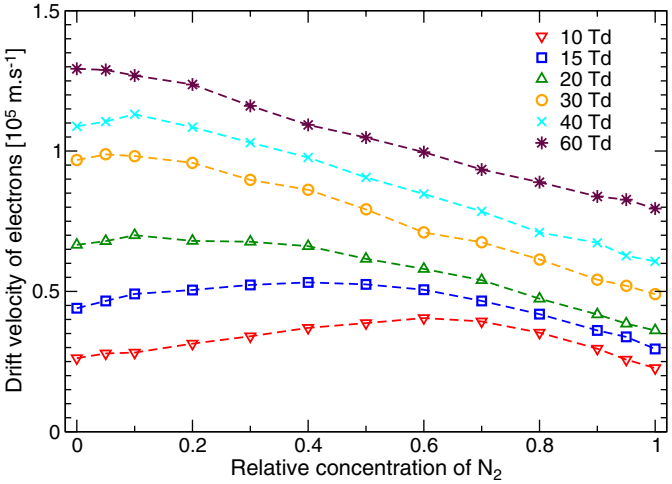

Fig. 3. The drift velocity of electrons in N_2/CO_2 mixture for $E/N < 80$ Td.

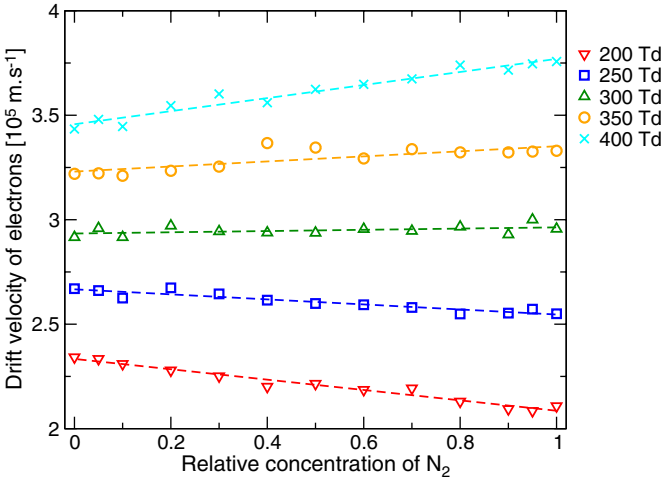

Fig. 4. The drift velocity of electrons in N_2/CO_2 mixture for E/N from 200 to 400 Td.

At 300 Td, the value of v_d was already almost constant in the whole range of δ_{N_2}. Above 300 Td, the value of v_d started to grow linearly with the increasing δ_{N_2} (Fig. 4).

3.4 Collision frequency of electrons with neutrals

For E/N below 40 Td, the dependence of ν on δ_{N_2} was strongly non-linear (Fig. 5), because low energy electrons were under the significant influence of the momentum transfer cross section of CO_2, i.e. they encountered a large number of elastic collisions. Therefore, in CO_2-dominant mixtures, the increase of E/N from 10 to 40 Td lead to the decrease of ν, since the number of elastic collisions decreased with the increasing energy of electrons. For $E/N > 40$ Td, ν grew again, but mainly due to the increasing number of inelastic collisions. The situation was different in N_2-dominant mixtures. Since the momentum transfer cross section for electron-impact collisions of electrons with N_2 is small for low energy electrons, ν grew monotonously with the increasing E/N.

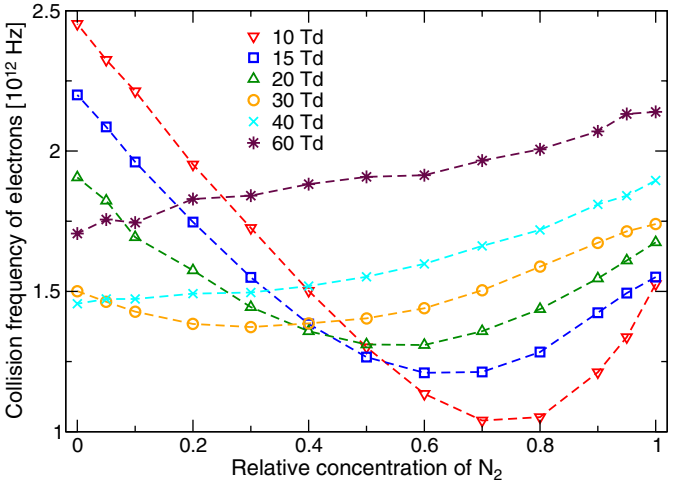

Fig. 5. The collision frequency of electrons with neutrals in N_2/CO_2 mixture for $E/N < 80$ Td.

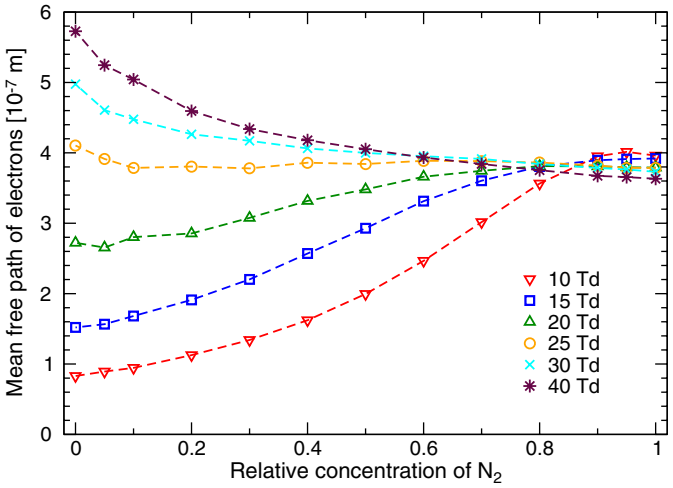

Fig. 6. The mean free path of electrons in N_2/CO_2 mixture for $E/N < 60$ Td.

For $E/N \geq 60$ Td, the influence of the momentum transfer cross section of CO_2 was small even in pure CO_2, and ν grew linearly with the increasing δ_{N_2}. It was therefore possible to fit ν for $E/N \geq 60$ Td according to equations (11–13).

3.5 Mean free path of electrons

The mean free path of electrons as a function of δ_{N_2} was non-linear in the whole region of E/N we dealt with. However, it was possible to fit λ with polynomials of the 3rd order for $E/N > 60$ Td. For $E/N \geq 40$ Td, λ decreased with increasing δ_{N_2}, but for $E/N < 40$ Td, the behaviour of λ as a function of δ_{N_2} was very complicated (Fig. 6). In mixtures with $\delta_{N_2} \geq 0.8$, λ was almost constant, it lied between 3.2×10^{-7} and 4.0×10^{-7} m for E/N ranging from 10 to 400 Td. With the increasing concentration of CO_2, λ varied more significantly as a function of E/N, caused by a large momentum transfer cross section of CO_2. And,

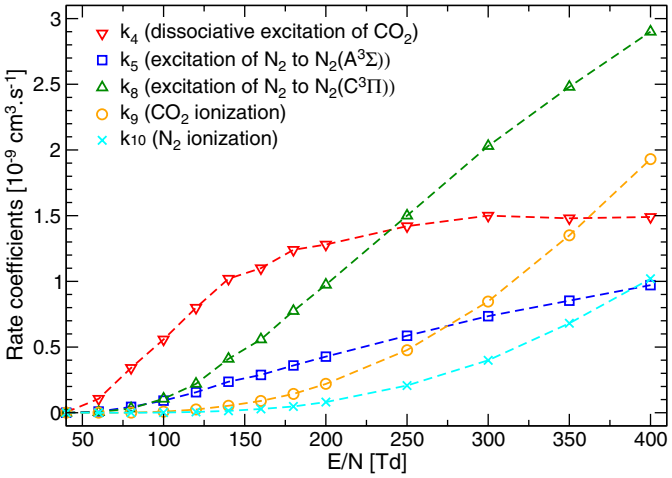

Fig. 7. The growth of rate coefficients with E/N in gas mixture with 50 vol.% N_2 ($\delta_{N_2} = 0.5$).

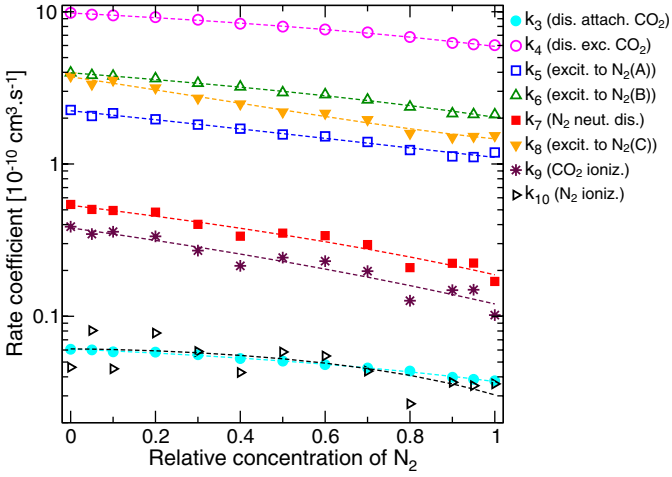

Fig. 8. Various rate coefficients as a function of N_2 concentration, at $E/N = 120$ Td.

as it was already mentioned, this influence was significant mainly for $E/N < 40$ Td. For $E/N \geq 40$ Td, λ changed only slightly also in the mixtures with high concentration of CO_2.

3.6 Rate coefficients of electron-impact reactions

The rate coefficients of electron-impact reactions as functions of E/N at constant δ_{N_2} performed three typical features (Fig. 7). Some rate coefficients grew exponentially with increasing E/N, e.g. k_9 and k_{10} for the ionisation of CO_2 and N_2, respectively. Other rate coefficients grew exponentially for $E/N < 80$ Td, and then almost linearly for higher E/N, e.g. k_5 and k_8 for the electron-impact excitations of N_2 in the ground state to states $N_2(A^3\Sigma_u^+)$ and $N_2(C^3\Pi_u)$, respectively. Finally, there are rate coefficients, which exhibited a logarithmic-like growth with the increasing E/N, with even a slight decrease for $E/N > 300$ Td, e.g. k_4 for the dissociative excitation of CO_2. However, the type of the growth of some rate coefficients changed with δ_{N_2}.

The influence of δ_{N_2} dominated below 80 Td, where all studied rate coefficients decreased exponentially with increasing δ_{N_2}. For $E/N > 80$ Td, they usually decreased linearly with the increasing δ_{N_2}. The slope of these curves depended on E/N and was specific for every rate coefficient. For k_3, k_9 and k_{10}, the slope even changed its sign for $E/N > 300$ Td, where these three rate coefficients increased linearly with the increasing δ_{N_2}, i.e. they exhibited behaviour similar to v_d (Fig. 4).

Figure 8 shows the rate coefficients of the studied electron-impact reactions as functions of δ_{N_2} at 120 Td. As can be seen, the dissociative excitation of CO_2 to the repulsive state $CO_2(a^3\pi)$ (k_4), and electronic excitations of N_2 (k_5, k_6, and k_8), were the fastest reactions. On the other hand, the dissociative attachment (k_3) and ionisation (k_9, k_{10}) were the slowest among these processes.

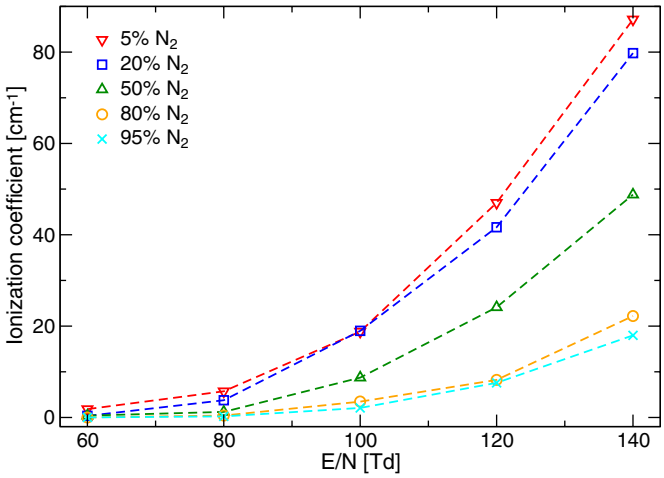

Fig. 9. Ionization coefficient in various N_2/CO_2 mixtures as a function of E/N.

3.7 Ionisation and attachment coefficients

Despite the dissociative attachment and ionisation were the slowest reactions, they are very important for the development, properties and stability of electrical discharges. Therefore, it is necessary to know their values as functions of E/N and δ_{N_2}. We found that the α and η increased with E/N for all δ_{N_2} ranging from 0.05 to 1. The growth of α was exponential (Fig. 9), whereas the growth of η was logarithmic (Fig. 10). For both α and η, the growth was steeper in the mixtures with higher concentration of CO_2. At the constant E/N, α and η grew with the decreasing δ_{N_2}.

4 Conclusions

Motivated by the decomposition of CO_2 and the synthesis of amino acids in DC electrical discharges, we investigated the electron dynamics by Monte Carlo simulations in N_2/CO_2 gas mixtures. The results of the simulations

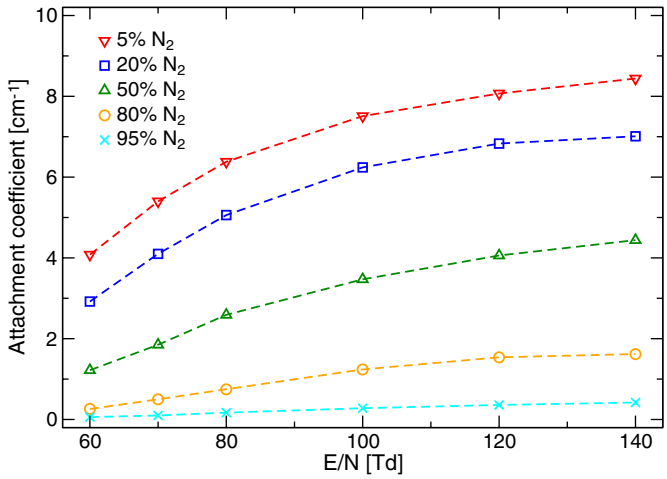

Fig. 10. Attachment coefficient in various N_2/CO_2 mixtures as a function of E/N.

include electron mean energy, drift velocity, collision frequency of electrons with neutrals, mean free path of electrons, rate coefficients of selected electron-impact processes, and ionisation and attachment coefficients as functions of the reduced electric field strength and the composition of a gas mixture. The knowledge of these parameters is crucial for the understanding of plasma induced chemistry and behaviour of electrical discharges in such mixtures.

For E/N below approximately 80 Td, the studied parameters were mostly non-linear functions of N_2 concentration (δ_{N_2}). Above 80 Td, these dependences were still often non-linear but they could be fitted by polynomials of up to the 3rd order. The fitting coefficients enabled the calculation of the studied parameters as functions of E/N and δ_{N_2} with high accuracy. The rate coefficients for electron-impact reactions with high ε_{th}, however, were fitted with high accuracy only for E/N above 140 Td. It is due to the statistics, since these rate coefficients are calculated only from the 'tail' of the EEDF. The EEDFs and the derived parameters were mostly influenced by elastic collisions and vibrational excitations. The elastic collisions prevailed for E/N below 40 Td in CO_2-dominant mixtures. For $E/N > 40$ Td, the influence of vibrational excitations of N_2 dominated. This influence was the strongest for E/N from 40 to 60 Td, and it decreased with the increasing E/N and with the decreasing concentration of N_2. The vibrational excitations also influenced the rate coefficients of electron-impact reactions, as they decreased with the increasing δ_{N_2}. However, the influence of the vibrational excitations on the rate coefficients weakened with the increasing E/N.

The applied computational method was proved useful for the calculation of steady-state EEDFs and derived parameters characterising electrons in homogeneous electric fields in various gaseous mixtures. However, we will warmly welcome any suggestions for its further development. Web-EEDF source code can be downloaded from `http://enviro.fmph.uniba.sk/web-eedf`.

This work was carried out under the support from Slovak Grant Agency VEGA 1/2013/05, 1/3041/06 and 1/3068/06; NATO EAP.RIG 981194, and Slovak Research and Development Agency APVT-20-032404, and APVV 0267-06 grants.

References

1. U. Kogelschatz, J. Salge, in *Low temperature plasma physics*, edited by R. Hippler, S. Pfau, M. Schmidt, K.H. Schoenbach (Wiley-VHC, Weinheim, 2001)
2. H.-H. Kim, Plasma Process. Polym. **1**, 91 (2004)
3. M. Laroussi, IEEE Trans. Plasma Sci. **30**, 1409 (2002)
4. C.-J. Liu, G.-H. Xu, T. Wang, Fuel Proc. Techn. **58**, 119 (1999)
5. Z. Machala, M. Morvova, E. Marode, I. Morva, J. Phys. D: Appl. Phys. **33**, 3198 (2000)
6. M. Cernak, J. Rahel, D. Kovacik, M. Simor, A. Brablec, P. Slavicek, Contrib. Plasma Phys. **44**, 492 (2004)
7. M. Morvova, I. Morva, M. Janda, F. Hanic, P. Lukac, Int. J. Mass Spect. **223**, 613 (2003)
8. K. Plankensteiner, H. Reiner, B. Schranz, B.M. Rode, Angew. Chem. Int. Ed. **43**, 1886 (2004)
9. T. Mikoviny et al., in *Proceedings of the 15th Symposium on Applications of Plasma Processes and 3rd EU-Japan Joint Symposium on Plasma Processing*, Podbanské, Slovakia, 2005, p. 213
10. M. Janda, Ph.D. thesis, Leopold Franzens University of Innsbruck and Comenius University Bratislava, 2006
11. D. Reiter, S Wiesen, M. Born, Plasma Phys. Control. Fusion **44**, 1723 (2002)
12. A.M. Runov, S.V. Kasilov, R. Schneider, D. Reiter, J. Plasma Phys. **72**, 1109 (2006)
13. S. Droste, D. Borodin, A. Kirschner, A. Kreter, V. Philipps, U. Samm, Contrib. Plasma Phys. **46**, 628 (2006)
14. A. Munoz, J.M. Perez, G. Garcia, F. Blanco, Nucl. Instrum. Meth. Phys. Res. A **536**, 176 (2005)
15. M. Braglia, Contrib. Plasma Phys. **32**, 497 (1992)
16. S. Hashiguchi, IEEE Trans. Plasma Sci. **19**, 297 (1991)
17. A.P. Palov, V.V. Pletnev, V.G. Telkovskii, Sov. J. Plasma Phys. **17**, 295 (1991)
18. K. Satoh, Y. Ohmori, Y. Sakai, H. Tagashira, J. Phys. D: Appl. Phys. **24**, 1354 (1991)
19. E.M. van Veldhuizen, Ph.D. thesis, Eindhoven University of Technology, 1983
20. H.R. Skullerud, Phys. D: Appl. Phys. **1**, 1567 (1968)
21. Y. Weng, M.J. Kushner, Phys. Rev. A **42**, 6192 (1990)
22. M. Yousfi, A. Himoudi, A. Gaouar, Phys. Rev. A **46**, 7889 (1992)
23. C.K. Birdsall, IEEE Trans. Plasma Sci. **19**, 65 (1991)
24. T.J. Sommeren, Plasma Sources Sci. Technol. **2**, 198 (1993)
25. P. Segur, M. Yousfi, M. Bordage, J. Phys. D: Appl. Phys. **17**, 2199 (1984)
26. M. Janda, Z. Machala, M. Morvova, V. Francek, P. Lukac, Acta Phys. Slov. **55**, 507 (2005)
27. M. Janda, `http://enviro.fmph.uniba.sk/web-eedf`
28. M.A. Tas, E. van Veldhuizen, W. Rutgers, J. Phys. D: Appl. Phys **30**, 1636 (1997)
29. M. Janda, K. Hensel, V. Martisovits, M. Morvova, Czech. J. Phys. **56**, B774 (2006)
30. `http://jilawww.colorado.edu/www/research/colldata.html`
31. Y. Itikawa, J. Phys. Chem. Ref. Data **31**, 749 (2002)
32. M. Mitchner, C. Kruger Jr, *Partially Ionized Gases* (John Wiley & Sons, Inc., New York, 1973)